

An Airspeed Vector Sensor for V/STOL Aircraft

Enoch Durbin*

Princeton University, Princeton, N.J.

and

Tad McGeert†

Stanford University, Stanford, Calif.

For some years a technique for airspeed sensing using the ion beam of the positive corona discharge has been under development at Princeton University. This technique employs ions in transit across an electrode gap; these may be deflected by airflow during their transit, and by measuring the deflection one can determine the flow rate. In most ion sensors the relationship is linear and very accurate, which makes this technique particularly suited to low speed sensing. With the specific requirements of V/STOL aircraft in mind, we have applied this technique to airspeed vector sensing, that is, simultaneous resolution and measurement of three airspeed components. Our research has led to a prototype sensor which has demonstrated the following characteristics in wind-tunnel tests: 1) a response to each flow component which is linear and virtually insensitive to temperature and humidity variations; 2) little coupling between the three responses; 3) a maximum measurable speed of 50 m/s, which may easily be increased; and 4) an accuracy on the order of 0.01-0.1 m/s. The sensor is fairly light, and has no moving parts. The paper includes discussion of the principles of the sensing technique, the testing of our prototype, and means for further refinement.

Introduction

ALL pilots, be they human or electronic, have a fundamental need for vector airspeed information. The accuracy and completeness needed in this information varies with the mission and the flight regime. It is particularly important in low speed maneuvering of helicopters and V/STOL aircraft, where optimum performance is achieved in a narrow speed range—a knot's error in the rotation speed of a heavily loaded helicopter, for instance, can incur significant penalties in payload and distance required to clear obstacles. Complete velocity information is often needed for safe as well as for optimum flight; on the Harrier, for example, sideslip must be held within a quite narrow band during hover and transition to avoid exceeding lateral control power. However, the requirement is not limited to low speed flight. It includes, for example, the takeoff and initial climb of a large transport, for which optimum rotation speed and climb angle of attack are also very well-defined quantities.

Aircraft most commonly use the pitot-static system to provide velocity information. This system is attractive because of its simplicity and unobtrusiveness, and works quite well provided that the aerodynamic angles are small and the speed is above 30 or 40 knots. At larger angles, however, its error becomes significant, while at low speeds it is essentially insensitive. Moreover, while the information it provides can be related to true airspeed by applying a density correction, and to angle of attack by a calculation involving aircraft gross weight and load factor, the system can sense only a single component of velocity. Flow angle vanes are needed to resolve the other two components; the sensitivity of these is also reduced at low speed, where inertial and frictional forces upon them are of the same order as the aerodynamic forces.

Because of the problems associated with this and other currently used techniques, there remains an outstanding need for an airspeed vector sensor. Such a device should be capable

of operating over the whole of the flight envelope. It should be insensitive to environmental variations, and preferably linear in response. It should be simple, robust, and sufficiently clean to hang on to an airframe.

We have recently developed at Princeton an ion beam anemometer which meets the requirements cataloged above, and so has the potential for satisfying this need. The device resolves a flow vector into three components and measures the components simultaneously. The response to each component is linear in velocity, and can be made insensitive to environmental variations.

The purposes of this paper are, first, to explain the sensor's principles of operation and, second, to present results obtained in trials of a prototype device. These are, respectively, the subjects of the following two sections.

The Ion Flow Revealed

The sensor does in fact use two related, but distinct, techniques for velocity measurement. One flow component is measured in what we refer to as axial sensing, while the two orthogonal components are measured in transverse sensing. The axial sensing technique is the simpler and more analytically tractable, and so it is natural to treat this method first. It is best illustrated by considering a single component sensor of the coaxial type, such as is shown in Fig. 1.

Axial Sensing

In an elementary form, this sensor is simply a central rod bearing a single needle—the anode—surrounded by a grounded cylinder, which is the cathode. If a voltage is placed on the rod, an electric field is established between the rod and the cylinder which is one-dimensional except in the vicinity of the needle. Near the needle there is an intense perturbation in the field, which at some very high voltage is sufficiently strong to cause the gap between the needle and the cylinder to break down, and a spark occurs. But below this voltage, ionization of the gas about the needle occurs without complete breakdown. This is the corona discharge. This process begins at the threshold voltage, which might typically be 4 kV for an electrode gap of 3 cm; current increases quadratically with voltage above this level. (A sensor of this type would normally operate at a current level of about 20 μ A.) The ions formed at the needle diffuse across the gap at a radial drift speed, V_{dr} , on the order of 50 m/s. Thus the transit time τ is on the order

Presented as Paper 80-1938 at the AIAA Conference on Sensor Systems for the 80's, Colorado Springs, Colo., Dec. 2-4, 1980; submitted Jan. 9, 1981; revision received Sept. 21, 1981. Copyright © American Institute of Aeronautics and Astronautics, Inc., 1981. All rights reserved.

*Professor, Department of Mechanical and Aerospace Engineering.

†Research Assistant, Department of Aeronautics and Astronautics. Member AIAA.

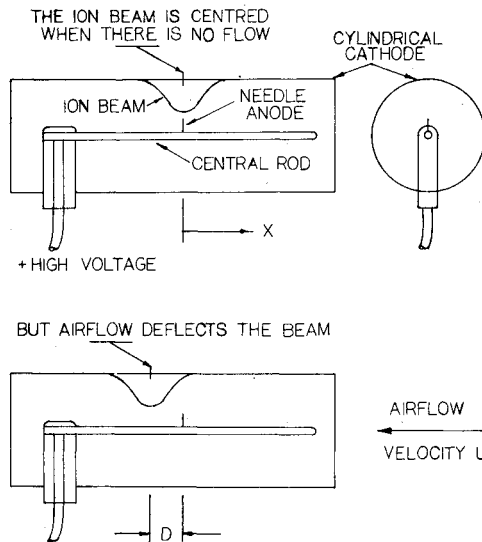


Fig. 1 Coaxial airspeed sensor.

of 0.5 ms. Mutual repulsion causes the ions to diffuse longitudinally as well as radially into a Gaussian distribution, whose mean is in the plane of the needle when there is no flow through the sensor. The distribution in this sensor would have a width, as measured by the "standard deviation" of the Gaussian distribution, of about 0.75 cm.

Consider a flow at speed U along the axis. The flow translates the current distribution downstream, but does not distort it provided that the longitudinal electric field about the needle is negligibly small. In this case, the electric field in the mean of the ion beam, which has both longitudinal and radial components, is unchanged by the flow. Therefore V_{dr} and τ are also unchanged. The deflection of the distribution's mean, D , is just the product of τ and U , and so is inherently linear in velocity.

Relationship of Deflection to Velocity

This relationship can be put on a quantitative footing as follows. If the anode and cathode radii are denoted by r_a and r_c , respectively, then the beam deflection may be written as

$$D = \int_{\tau} U d\tau = \int_{r_a}^{r_c} \frac{U dr}{V_{dr}} \quad (1)$$

Before this integral can be evaluated, V_{dr} must be expressed as a function of r . The first step in this direction is to eliminate V_{dr} in favor of the radial electric field strength, E_r . In fact, the drift velocity of an ion through a neutral gas is linearly related to the electric field E through the formula

$$V_d = \mu E \quad (2)$$

Here μ is the so-called ion mobility. It has a value of about $1.9 \text{ cm}^2/\text{V-s}$ at room temperature. Notice that weak fields such as are used in this sensor produce a velocity rather than an acceleration. This is because the ions, whose numbers are small compared to the total number of particles in any region (about 1 in 10^{10}), lose the momentum acquired from the electric field after each collision—on average, therefore, after each transit of a mean free path. Mobility thus varies with the mean free path and, consequently, with gas composition and state. A particularly significant corollary is that mobility is inversely proportional to density.

From this formula it follows that the drift velocity in the radial direction is given by

$$V_{dr} = \mu E_r \quad (3)$$

Substitution of this expression into the integral above gives

$$D = \int_{r_a}^{r_c} \frac{U dr}{\mu E_r} \quad (4)$$

Now, if E_r can be expressed as a function of r , then this integral can be evaluated to obtain a simple equation for the beam deflection D .

The field E_r has two components. The first is the surface charge field, which is due to the voltage on the anode rod. The second is the space charge field, which is due to mutual repulsion within the ion beam. Both of these components are included in the following expression, developed by Burke,¹ for the radial field in the mean of the ion distribution:

$$E_r(r, \mu) = \left[\frac{2i\bar{A}(r, \mu)r}{\mu\epsilon A^2(r, \mu)} + \left(\frac{V_t}{r \ln(r_c/r_a)} \right)^2 \right]^{1/2} \quad (5)$$

The second term is the surface charge contribution to the field. V_t is the threshold voltage, that is, the voltage at which ionization begins. Its value depends upon the geometry of the sensor and upon rather subtle characteristics of the needle, and, for a given needle and sensor geometry, has been found to vary inversely as the square root of μ .

The first term contains the space charge contribution. The total current is represented by i ; ϵ is the dielectric constant of the neutral gas; $A(r, \mu)$ is the area of the ion beam at radius r , and \bar{A} is the mean area up to that radius.

As yet this expression cannot be used in the deflection integral, since the functions $A(r, \mu)$ and $\bar{A}(r, \mu)$ are not written explicitly in terms of r . The formulation was completed by Weatherspoon,² who derived the following relationship empirically:

$$A = 2\pi k \mu r^3 \quad (6)$$

Here k is a constant determined by the geometry of the device. With this formula in hand, one can proceed with the deflection integral. A particularly significant result is obtained if the surface charge component of the electric field is assumed to be negligible compared with the space charge component; in practice this situation is achieved by ensuring a relatively low threshold voltage and operating at a relatively high current level. The beam deflection in this case is

$$D = (r_c^2 - r_a^2) (k\pi\epsilon/i)^{1/2} U \quad (7)$$

The practical importance of this result is that μ —the significant parameter in determining the sensitivity of the device to environmental variation—does not appear. Thus, if the sensor is operated at a sufficiently high current level that the surface charge field becomes negligible in comparison with the space charge field, then its response will be insensitive to environmental variations.

On the other hand, if the current is sufficiently low that the space charge field is negligible, then this convenient elimination of the ion mobility does not occur; a factor of $\mu^{1/2}$ remains in the denominator of the equation (after the variation of the threshold voltage with mobility is taken into account). Therefore, in this case, the sensor's calibration constant will change as the ambient conditions vary.

The physical processes which underlie these relationships should be described. Consider operation at a constant current level which is so low that the surface charge field is dominant. In this case the ions move in proportion to the surface field strength and their own mobility. Since $V_{dr} = \mu E_r$, one would at first glance expect an increase in mobility to produce a proportional increase in the ions' drift velocity, and an associated decrease in their transit time. But remember that the voltage required to generate any given current decreases with increasing mobility; therefore the source voltage must be

lowered if the current is to remain constant. This reduces the radial field strength, so that the ions move faster only in proportion to $\mu^{1/2}$, rather than to μ itself. The transit time, and so the deflection per unit velocity, are reduced by the same factor.

A space charge dominated field weakens even more rapidly with mobility; this occurs as follows. The space charge field depends upon the ion beam width. The beam width depends upon the ions' diffusion rate. Increasing the mobility encourages diffusion; this spreads the beam, which, in turn, reduces the space charge field. It turns out that the reduced radial field strength exactly cancels the increased mobility in determining the drift velocity, and so the transit time remains unchanged.

The foregoing analysis makes these two fundamental points:

- 1) Beam deflection is linear in velocity regardless of current level.
- 2) Provided that the current is sufficiently large, the beam width varies with mobility in such a way that beam deflection becomes insensitive to environmental change.

Measurement of the Beam Deflection

Thus the beam deflection, or, more precisely, the position of the mean of the current distribution, is a convenient indicator of the flow rate through the sensor. It is, of course, the figure of interest in flow sensing. To locate the mean of the ion beam, one must evaluate the integral

$$\langle x \rangle = \int_{-\infty}^{\infty} x j(x) dx \quad (8)$$

Here, $j(x)$ is the current density (normalized by the total current) at some point x along the axis of the sensor. This integration can be performed simply and precisely by using a resistive cathode—such as, for example, a strip of resistive film bonded to the inner wall of the cylinder, and tapped at each end. If the cathode has uniform resistance per unit length, then it divides the current collected about any longitudinal position to the left and right in inverse proportion to the distance from each end. It thus performs the necessary weighting of the current distribution by x , so that the integral is exactly equal to the difference between left- and right-hand currents, normalized by their sum— $\Delta i/i$ in shorthand notation.

Of course, some degree of approximation to perfectly uniform cathode resistance can be made, and in fact rather crude approximations are quite acceptable in practice. Thus a cathode composed of a series of discrete segments connected by resistors, rather than a uniform resistive film, can be used. Provided that the width of each segment is small compared to the width of the current distribution—say, less than one "standard deviation" width—the calculation of the deflection integral performed by such a cathode is only negligibly in error.

Moreover, just as this technique for airflow sensing can be used in various coaxial configurations, so also can it be broadly applied to completely different geometries—linear (i.e., rod), planar, and cylindrical cathodes can be used. Only a constant electrode gap perpendicular to the sensitive axis, a cathode which is essentially continuous along the axis, and a source located in a single transverse plane are required. However, the cylindrical variety is the most practical as it permits effective masking of the longitudinal field about the source needle. As will be seen, this field causes skewing of the current distribution with flow, and nonlinearity can result if the skewing is excessive.

The technique used in all of these configurations is referred to as axial, or longitudinal, sensing. Its attributes are inherent linearity; insensitivity to environmental variations at high current; and range which can, in principle, be extended indefinitely simply by extending the cathode downstream.

Transverse Sensing

A second technique, transverse sensing, can be used to measure flows in the plane of, rather than perpendicular to, the radial ion drift. The elements of this technique can be appreciated by again considering a coaxial configuration. However, in this case the cathode must be an open mesh, which allows flow across the x axis to pass through the sensor effectively undisturbed. For clarity, assume also that the current distribution is uniform over the circumference of the cathode when there is no flow through the sensor. Now, consider the effect of introducing a transverse flow. This produces a transfer of current from the windward to the leeward side of the sensor, which makes the circumferential current distribution asymmetric. By sensing the magnitude of the asymmetry, one can obtain a measure of the flow rate.

Transverse sensing, then, involves lateral, rather than longitudinal, current transfer within the sensor, and so is physically quite different from axial sensing. But it has similar attributes nonetheless. Weatherspoon² was the first to demonstrate linearity and insensitivity to environmental change at high current using the technique. Moreover, this method inherently allows measurement of two flow components, simply by sensing the magnitude of the asymmetry across orthogonal axes in the transverse plane. (The asymmetry across each axis may be expressed as a difference between upstream and downstream currents over the total; thus the output, $\Delta i/i$, is of the same form as in axial sensing.)

Transverse sensing therefore has an advantage over axial sensing in being able to sense two flow components, but, on the other hand, it does not have the (in principle) unlimited range of axial sensing. At some speed, virtually all of the current is collected on one side of the sensor, and saturation occurs. Consequently, one can extend the range only by increasing the current level or by reducing the electrode gap (i.e., by reducing the transit time). We have found empirically that, while these are effective, they are not quite so powerful as in axial sensing. Specifically, the governing relationships seem to be the square roots of those which apply in axial sensing—transverse sensitivity ($\Delta i/i$ per unit velocity) apparently varies linearly with radius, rather than with its square, and inversely with the $1/4$, rather than the $1/2$, power of the total current.

That is not to say that the range in transverse sensing is impractically small. A maximum measurable speed of at least 50 m/s is typical; this is certainly adequate for the intended purpose. In fact, a sensor in which the two techniques of transverse and axial sensing are combined seems ideal for use on aircraft. Such a device has a relatively large speed range along its longitudinal axis, and a lesser range along its lateral axes; this is, of course, also true of any aircraft which has a reasonable maximum speed in any direction. This synthesis of the transverse and axial sensing techniques is the essence of the design described here.

Experiments with a Prototype Device

The preceding section has introduced in both qualitative and quantitative terms the two sensing techniques, axial and transverse, which are used to resolve and measure the components of an airspeed vector. This section deals with our experimental results, which illustrate the application of these techniques. These results were obtained with a device which was christened the Mark IV, as it was approximately the fourth in a series of prototypes of diverse configurations. Its configuration was coaxial, with an open cathode structure designed to allow flow from any direction to pass unobstructed through the sensor.

In order to follow this discussion, one must have in mind a clear picture of the sensor's axis system and the conventions for defining flow directions with respect to it. Therefore a description of these conventions is in order at this point.

The x axis corresponds to that of the coaxial sensor described previously. If the x axis points forward, then the y axis points to the left, and the z axis points upward, from an

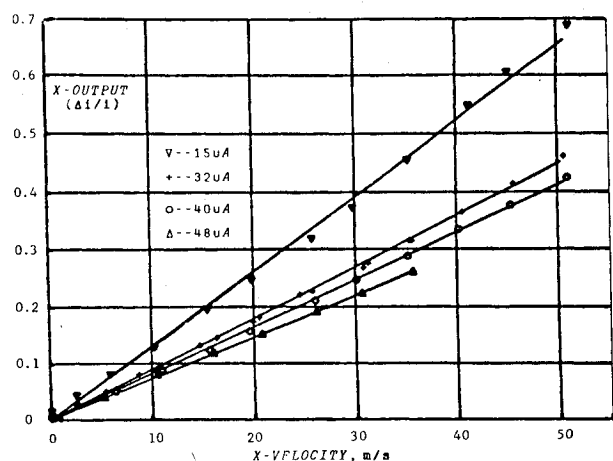


Fig. 2 x output vs x velocity at various current levels.

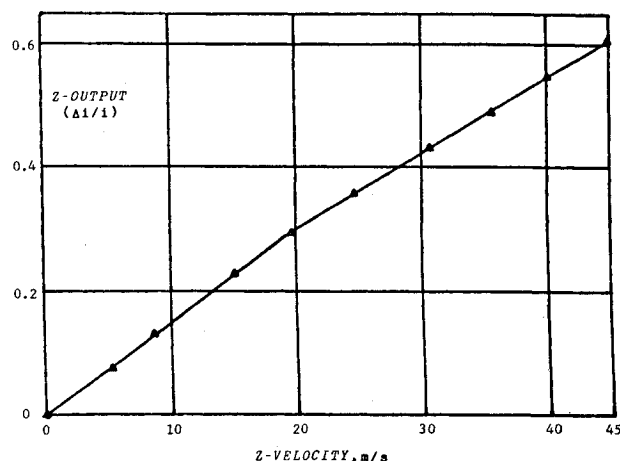


Fig. 4 z output vs z velocity at $32 \mu\text{A}$ total current.

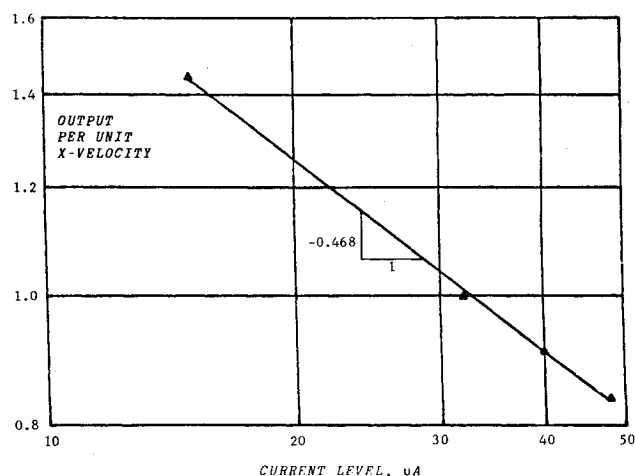


Fig. 3 Output per unit x velocity as a function of current level. The ordinate has been normalized to 1 at a current level of $32 \mu\text{A}$.

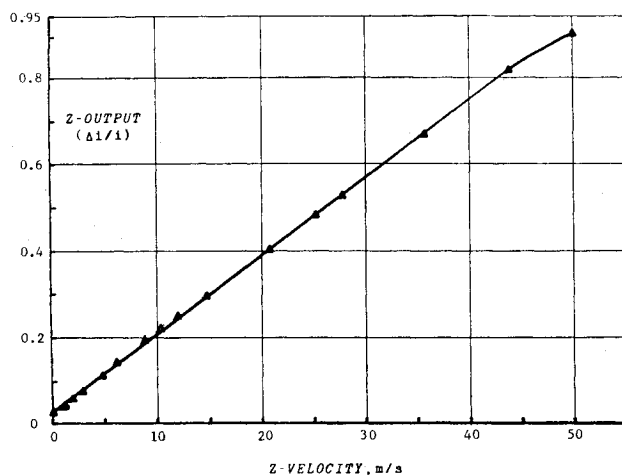


Fig. 5 Transverse response of the Mark II sensor ($20 \mu\text{A}$ total current).

origin coincident with the ion source. The sign convention is that flows from positive to negative along each axis are positive; thus flow from forward, leftward, and above the sensor has positive x , y , and z components.

Transverse flow is parallel to the y - z plane. The angle of flow in this plane is referred to as the roll angle ϕ , measured so that positive z flow corresponds to $\phi=0$, and positive y flow to $\phi=90$ deg. The angle of flow in the x - z plane is referred to as the pitch angle α . Flow down the x axis corresponds to $\alpha=0$; α is positive if the flow through the sensor is upward.

This brief treatment of terminology should see the reader through the discussion of this section. Sensing of purely axial flow (i.e., flow having only an x component) will be treated first, followed by purely transverse flow. Finally, results of tests in combined transverse and axial flow will be presented.

Axial Response

The axial response of the Mark IV at various current levels is plotted in Fig. 2. Linearity is quite good except at $15 \mu\text{A}$. The eccentricity in that case is evidence of skewing in the current distribution, produced by the longitudinal electric field about the needle; this effect was alluded to earlier. At the higher current levels, this field was masked by more concentrated space charge near the anode.

The axial sensitivity (i.e., the slope of each response) is plotted against current level in Fig. 3. Weatherspoon's formulation [Eq. (6)] indicates that, if the electric field is dominated by space charge, then sensitivity will vary as the inverse square root of current level; this would give the plot a

slope of -0.5 . The measured slope is just a bit less (absolutely): -0.468 . One would, in fact, expect to measure less than -0.5 even in a purely space charge field, for Weatherspoon's formulation neglects a slight widening of the ion beam with increasing current. This effect moderates the variation of electric field strength, and therefore transit time, with current level. Actually the measured relationship between sensitivity and current level is about as strong as one could expect to realize in practice. Consequently, one can conclude from this result that the ions are moving in a strongly space charge dominated field, which, the reader will recall, is the condition for insensitivity to environmental change. Although we have not yet been able to test the effect of environmental change directly, insensitivity has been demonstrated in sensors of sundry other configurations operating with an equally strong space charge field. Therefore it is reasonable to anticipate that the outcome of such tests will be favorable.

Transverse Response

Figure 4 shows the response of the sensor to flow directed along the z axis. The response is linear below and above an output level of 0.3; however, the slope of the response changes at that point. This appears to be an aberration peculiar to the Mark IV, caused by four longitudinal supports placed inside the cathode. These introduced local reductions in the cathode radius, which in turn produced local strengthening of the electric field, and, ultimately, a perturbation in the rate of current transfer in transverse flow.

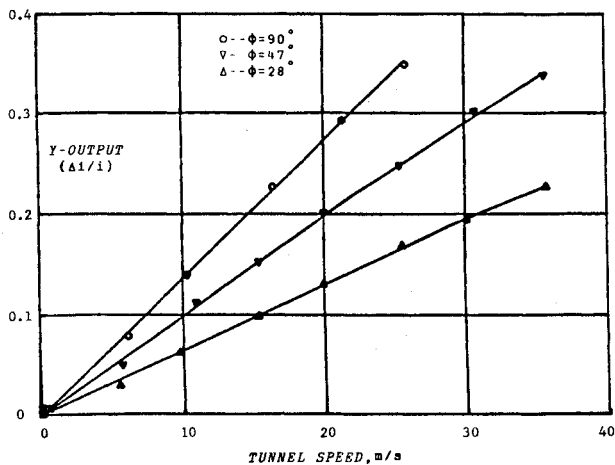


Fig. 6 y output vs tunnel speed at various roll angles ($48 \mu\text{A}$ total current).

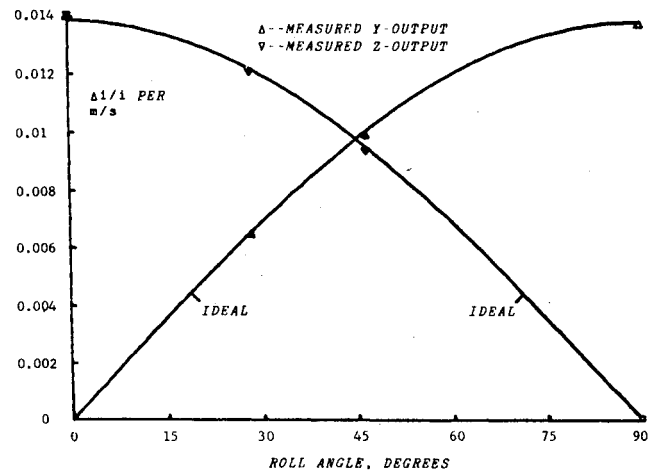


Fig. 8 Variation in y and z outputs with roll angle.

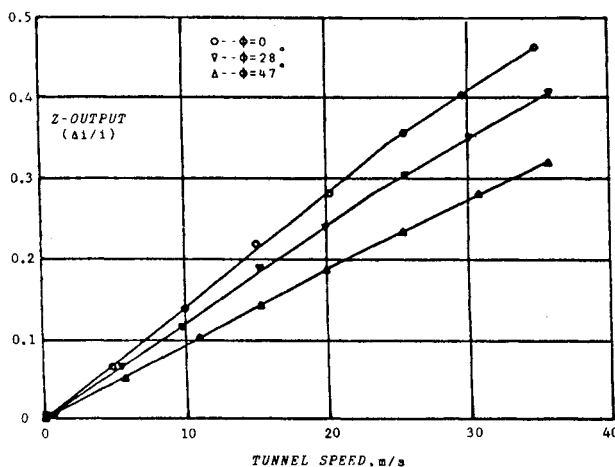


Fig. 7 z output vs tunnel speed at various roll angles ($48 \mu\text{A}$ total current).

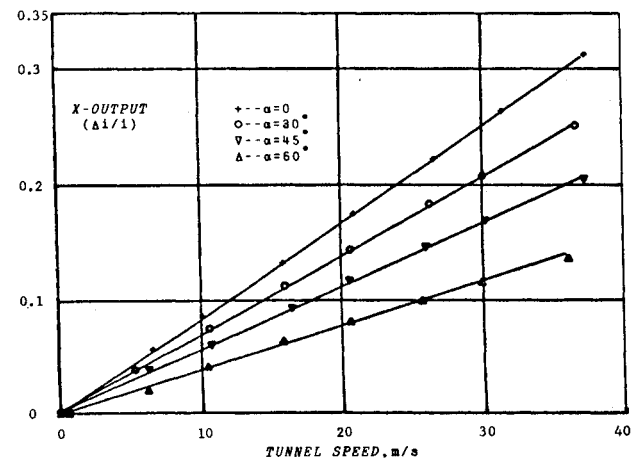


Fig. 9 x output vs tunnel speed at various pitch angles ($32 \mu\text{A}$ total current).

This aberration could almost certainly be eliminated by removing the supports to the outside of the cathode. Unfortunately, we were not prescient enough to realize this before building the Mark IV, and time has not allowed us to make the necessary modification. However, data which illustrate the expected effect are plotted in Fig. 5. These were obtained in transverse flow tests of an earlier mark of the sensor which had no such geometric peculiarities. The response is linear until the onset of saturation at $\Delta i/i \approx 0.85$. (It should be mentioned that the earlier sensor had an axial response which was not as good as that of the Mark IV; we anticipate that the Mark V will provide the best of both worlds!)

The nonlinearity is the only apparent adverse feature of the Mark IV's transverse response. It is rather adept at component resolution. Figures 6 and 7 show the variation in y and z outputs with roll angle. These should vary with the sine and cosine of ϕ , respectively. In Fig. 8, the initial slopes of these responses are plotted against ϕ , along with reference sine and cosine curves. Their coincidence is quite good. This result is as expected—the current differential along each axis is indeed dependent only upon the magnitude of the corresponding transverse component, and is not affected by the magnitude of the orthogonal component.

Combined Axial and Transverse Response

The sensor's characteristics in pure axial and pure transverse flow have now been described. Here the discussion turns to combination of the two. In particular, consider the case of

combined x and z flow produced by pitching the sensor about the y axis.

The axial response at various pitch angles (and zero sideslip) is plotted against tunnel speed in Fig. 9. Although each set of points in the figure is shown with a linear least-squares fit, the reader should note that at nonzero pitch angles there is a slight downward concavity in the responses. The curvature becomes more apparent when the responses are plotted against the X component of tunnel speed, as in Fig. 10. The nonlinearity reveals a "transverse-to-axial" coupling effect. This coupling effect has two causes.

The first and most easily remedied cause is that the cathode of the Mark IV was too short. Transverse flow increases the current density on one side of the sensor. The greater concentration of space charge there then increases mutual repulsion and this, combined with the otherwise negligible skewing produced by the needle, widens the ion beam on the downstream side. Thus, although the static edge-to-edge beam-width was only about 5 cm, at 50 m/s and, for example, a pitch angle of 45 deg, as much as 1 or 2% of the beam ran off the cathode, while the mean was still 5 cm from the end. The resulting error in the calculation of the mean deflection is of the same order as the current overflow.

This, however, is only a part of the problem, for our measurements indicate that the lost current does not account for the whole of the observed change in sensitivity. The remainder must be caused by a change in transit time. One could well anticipate such a change. Transverse flow increases the transit time of the ions collected upstream and reduces the

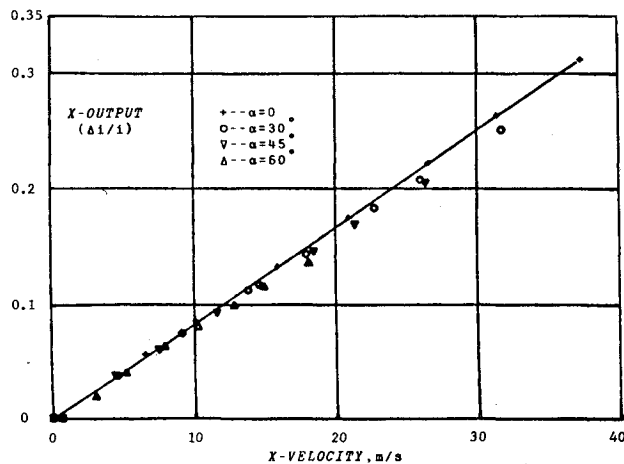


Fig. 10 x output vs x velocity at various pitch angles ($32 \mu A$ total current).

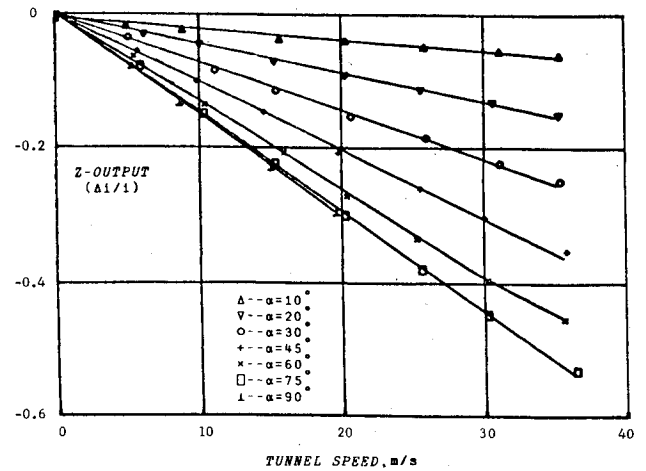


Fig. 12 z output vs tunnel speed at various pitch angles ($32 \mu A$ total current).

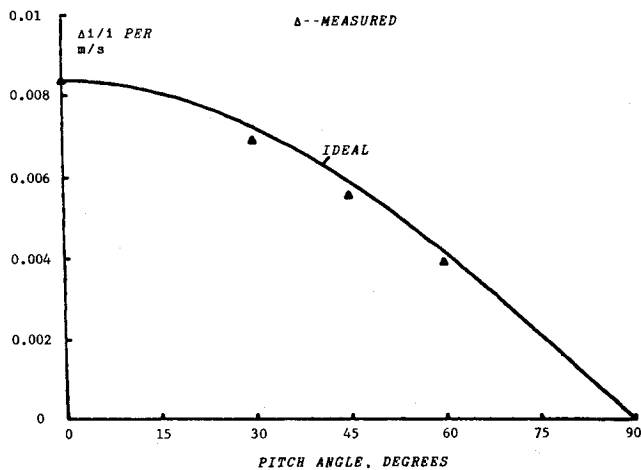


Fig. 11 Variation in x output with pitch angle.

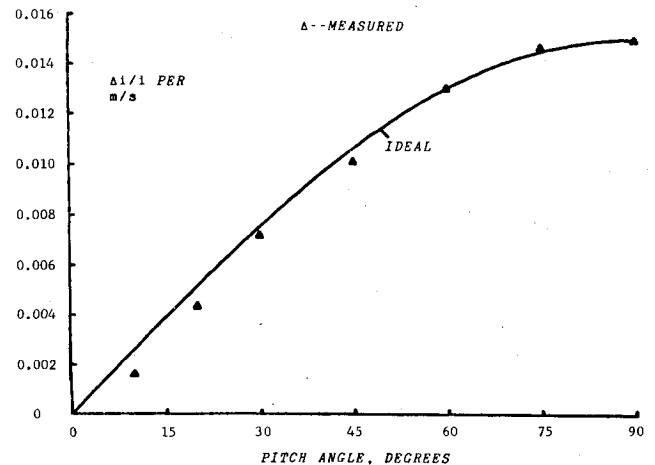


Fig. 13 Variation in z output with pitch angle.

transit time of those collected downstream—the change is due not only to the direct convective effect but also to a change in the space charge field. It would be very fortunate if the average transit time were to emerge from this process unscathed.

We are uncertain of the magnitude of the change in the Mark IV, as these data do not reveal how much error is due to current loss. Some indication, though, is provided by Fig. 11, in which the slopes of the least-squares fits in Fig. 9 are plotted with a reference cosine curve. The plot indicates that the axial sensitivity is reduced by about 4% at $\alpha = 30$ deg, and by about 6% at $\alpha = 45$ and 60 deg. If one attributes some of this effect to current loss, then one can conclude that the maximum change in transit time is about 5% over the range of speeds and flow angles explored.

An error of 5% can hardly be tolerated in a practicable sensor, so something should be done about this. Naturally, the preferred course of action would be to eliminate or substantially reduce the physical effect. Some improvement in this direction can certainly be achieved by changing the geometry of the sensor; whether this will reduce the effect to a negligible level will be determined by further experiments. If not, then calibration of the sensor's axial output will be necessary.

In combined flow the axial response is, of course, only part of the sensor's output. Consider now the variation of the transverse response with pitch angle. This is shown in Fig. 12. Note that positive pitch produces a negative z output according to the chosen sign convention. The slopes of these responses are plotted against α in Fig. 13 with a reference sine

curve. They correspond correctly except at small angles, where the discrepancy is probably due to incorrect measurement of the sensor's pitch angle. (Precise measurement of the pitch angle was difficult because of variations in the direction of flow through the tunnel.) These data, then, lead one to conclude with fair confidence that there is no "axial-to-transverse coupling," even though there is the converse interference.

The foregoing discussion has dealt with a special case of combined flow, namely, flow having components along only the x and z axes. But, in fact, a completely general flow, having x , y , and z components, is no more general as far as the sensor itself is concerned. Because of the sensor's axisymmetry, the current transfer process is the same regardless of the angle of flow in the transverse plane. Thus, if there is no axial-to-transverse coupling at zero roll angle, then there is none at any roll angle. The nonlinearity in the axial response is similarly independent of roll angle; it depends only upon the ratio of the magnitudes of the transverse and axial flows. These characteristics were verified in three-component flow sensing with the Mark IV.

Summary

We have discussed the theory of ion beam anemometry, the operation of an airspeed vector sensor which uses this technique, and the tunnel testing of a prototype device. The capabilities of a sensor of this type may be summarized as follows:

1) It resolves a general airspeed vector into one axial (x) and two transverse (y and z) flow components.

2) The response to each transverse flow component is linear, insensitive to environmental changes, and uncoupled from the orthogonal flow components.

3) The response to a pure axial flow is also linear and insensitive to environmental changes. The response to the axial component of a general airspeed vector, however, exhibits a small nonlinearity due to coupling. The coupling is a function of the magnitude of the airspeed vector, and the ratio of its axial and transverse components.

This "transverse-to-axial" coupling spoils what would otherwise be an ideal response; however, we should recognize that it does not introduce an ambiguity into the response. That is, the three outputs still specify an airspeed vector uniquely. So, given the coupling function, one could determine that vector by suitably processing the sensor's signals. Nevertheless, one would of course prefer to eliminate the coupling rather than correct for it. Since the coupling is already quite small, and since some of our current work indicates that it can be reduced, this seems a reasonable ambition.

In addition to the features enumerated above, the sensor has a range—easily greater than 100 m/s in the axial component and 50 m/s in the transverse components—which is well suited to aircraft. It has no moving parts, is reasonably compact and unobtrusive, and (the authors can attest) is surprisingly tolerant of imprecision in manufacture. We hope that, on the strength of these characteristics, and refinements which may be expected from further research, the device will be useful both on aircraft and in other applications.

References

¹Burke, W., "Air Speed Measurement with the Ion Beam of the Positive Corona Discharge," Ph.D. Dissertation, Princeton University, Department of Aerospace and Mechanical Sciences, 1972.

²Weatherspoon, S., "A Flow Vector Sensitive Ion Beam Anemometer," M.S.E. Thesis, Princeton University, Department of Aerospace and Mechanical Sciences, 1972.

³Durbin, E. and Born, G., "A New Mass Flow Measuring System Applicable to Aircraft Speed Measurement Including V/STOL," *Instrumentation in the Aerospace Industry*, Vol. 16, 1970.

From the AIAA Progress in Astronautics and Aeronautics Series..

AEROACOUSTICS:

JET NOISE; COMBUSTION AND CORE ENGINE NOISE—v. 43

FAN NOISE AND CONTROL; DUCT ACOUSTICS; ROTOR NOISE—v. 44

STOL NOISE; AIRFRAME AND AIRFOIL NOISE—v. 45

ACOUSTIC WAVE PROPAGATION;

AIRCRAFT NOISE PREDICTION;

AEROACOUSTIC INSTRUMENTATION—v. 46

Edited by Ira R. Schwartz, NASA Ames Research Center, Henry T. Nagamatsu, General Electric Research and Development Center, and Warren C. Strahle, Georgia Institute of Technology

The demands placed upon today's air transportation systems, in the United States and around the world, have dictated the construction and use of larger and faster aircraft. At the same time, the population density around airports has been steadily increasing, causing a rising protest against the noise levels generated by the high-frequency traffic at the major centers. The modern field of aeroacoustics research is the direct result of public concern about airport noise.

Today there is need for organized information at the research and development level to make it possible for today's scientists and engineers to cope with today's environmental demands. It is to fulfill both these functions that the present set of books on aeroacoustics has been published.

The technical papers in this four-book set are an outgrowth of the Second International Symposium on Aeroacoustics held in 1975 and later updated and revised and organized into the four volumes listed above. Each volume was planned as a unit, so that potential users would be able to find within a single volume the papers pertaining to their special interest.

v. 43—648 pp., 6 x 9, illus.	\$19.00 Mem.	\$40.00 List
v. 44—670 pp., 6 x 9, illus.	\$19.00 Mem.	\$40.00 List
v. 45—480 pp., 6 x 9, illus.	\$18.00 Mem.	\$33.00 List
v. 46—342 pp., 6 x 9, illus.	\$16.00 Mem.	\$28.00 List

For Aeroacoustics volumes purchased as a four-volume set: \$65.00 Mem. \$125.00 List

TO ORDER WRITE: Publications Dept., AIAA, 1290 Avenue of the Americas, New York, N.Y. 10019